The Chemistry of Dichloromethane Destruction in Atmospheric-Pressure Gas Streams by a Dielectric Packed-Bed Plasma Reactor

C. Fitzsimmons, F. Ismail, J. C. Whitehead,* and J. J. Wilman

Department of Chemistry, University of Manchester, Manchester M13 9PL,U.K.

Received: January 28, 2000; In Final Form: April 21, 2000

The destruction of dichloromethane by a nonthermal plasma in atmospheric-pressure gas streams of nitrogen with variable amounts of added oxygen has been investigated. The identities and concentrations of the end products are determined by on-line FTIR spectroscopy, and the plasma chemistry is interpreted using a kinetic modeling scheme. Peak destructions of 20% are found for a deposited energy of 66 J L^{-1}. The maximum dissociation is found for a carrier gas that contains 1−3% O_2, and the dissociation is greater in pure nitrogen than in an air stream. The major end products of the processing are HCN, Cl_2, and HCl in pure nitrogen and CO, $COCl_2$, HCl, and Cl_2 for gas streams containing oxygen. The plasma processing in streams containing oxygen also produces significant yields of nitrogen oxides. The mechanism of dichloromethane destruction in the plasma is predominantly oxidation initiated by atomic chlorine that is produced by collisions of dichloromethane with electronically excited nitrogen atoms and molecules. Because of low cross sections, electron attachment does not play a role in the destruction of dichloromethane. The addition of oxygen to the gas streams initially causes additional destruction from O and OH reactions, but further increase in the oxygen concentration causes inhibition of both the atomic chlorine cycle and the formation of NO_x and a consequent reduction in dichloromethane destruction.

Introduction

Nonthermal plasma processing is now being accepted as a proven technology for the removal of small concentrations (<2000 ppm) of volatile organic compounds from atmospheric-pressure waste-gas streams in addition to the more established technologies of catalytic oxidation, thermal decomposition, carbon adsorption, and condensation. Chlorinated solvents represent particularly difficult species to decompose, and any remediation method must ensure that the end products of the processing can be safely vented to the atmosphere or easily removed from the gas stream by precipitation or scrubbing. A variety of nonthermal, atmospheric-pressure, plasma methods such as electron beam,[1] pulsed corona,[1,2] capillary-tube discharge,[3] dielectric barrier,[2,4−8] dielectric packed-bed,[9−12] and hybrid plasma-catalyst methods[13] have been employed for the treatment of species such as methyl chloride,[5] dichloromethane,[9,14] carbon tetrachloride,[1,13,10] trichloroethane,[3] trichloroethene,[2−4,6,11,8,12] and chlorobenzene.[5,7]

In this paper, we report results from an investigation of the destruction of dichloromethane in a dielectric packed-bed reactor in which we identify the end products in real time using FTIR spectroscopy and vary the oxygen content of the gas stream. The experimental results are interpreted by means of kinetic modeling. The main thrust of the work is to elucidate the chemical mechanism of the destruction of the dichloromethane leading to the observed end products and to understand how this depends on the reactive species formed in the plasma. The majority of the previous studies have focused on the efficiency of the destruction process in terms of the electrical properties of the discharges and gas flows. The dielectric pellet-bed reactor is a variant of the more traditional dielectric barrier discharge reactor, or "silent discharge", long used for the generation of ozone.[15] A flow of gas passes through a tubular reactor packed with pellets of a dielectric material (barium titanate beads, in the present experiments) contained between two metallic electrodes. A high-frequency AC electric field is applied across the electrodes, causing the pellets to become polarized on each half-cycle, forming an intense electric field around each pellet contact point and resulting in a partial discharge.[16] The partial discharge consists of many short-duration (<100 ns) microdischarges. This allows the formation of a plasma whose components are not in thermal equilibrium and cannot be described by a single temperature. The deposited electrical energy produces very energetic electrons, while the gas remains near to its ambient temperature.[17] In a discharge of predominantly air, reactive species such as ground- and excited-state nitrogen and oxygen atoms and electronically and vibrationally excited oxygen and nitrogen molecules are formed. It is these species that drive the subsequent chemistry. With gas streams that contain halogenated species, electron attachment may become an important process in the plasma chemistry.

Experimental Section

The experimental arrangement is essentially the same as that employed previously.[18] A schematic diagram of the arrangement is shown in Figure 1. The pellet-bed reactor consists of a glass tube of 24-mm internal diameter with two electrodes ∼25 mm apart through which the gas passes. The space between the electrodes is packed with 3.5-mm-diameter barium titanate beads. The diameter of the beads is chosen to allow for as large a number of beads as possible (∼315), thereby maximizing the number of contact points for the formation of discharges while not restricting the porosity of the reactor significantly. This balances the requirements of having gas flow and as uniform a discharge as possible. An AC voltage (V_{pk-pk} = 0−30 kV) at a frequency between 10.25 and 13.25 kHz is applied between the electrodes. A mixed flow (0.3−10 L min^{-1}) of zero air and

* Author to whom correspondence should be addressed. E-mail: j.c.whitehead@man.ac.uk.

10.1021/jp000354c CCC: $19.00
Published on Web 06/03/2000

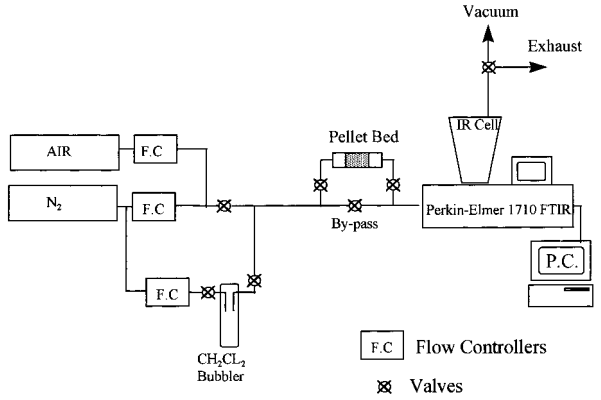

Figure 1. Schematic diagram of the arrangement used to study the plasma treatment of a gas flow of CH_2Cl_2 in a nitrogen/oxygen gas stream using a dielectric pellet-bed reactor.

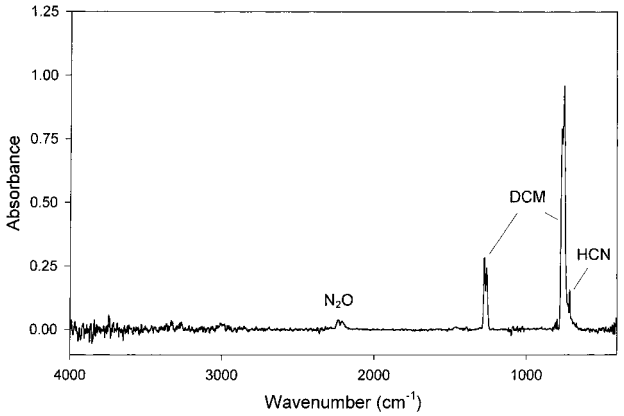

Figure 2. Medium-resolution (2 cm^{-1}) infrared spectra for an initial mixture of 500 ppm CH_2Cl_2 (DCM) in pure nitrogen at atmospheric pressure after processing in a dielectric pellet-bed reactor. The discharge conditions were $V_{pk-pk} = 15$ kV, frequency = 10.0 kHz, and flow rate = 1 L min^{-1}. The path length for the infrared gas cell was 2.12 m.

nitrogen controlled by flow controllers (MKS Mass Flo) is passed over solid dichloromethane at approximately −20 °C, in a salt-ice bath, giving an approximate concentration of 500 ppm of CH_2Cl_2 entering the plasma reactor. The gas mixture was maintained at a pressure of 1 bar. For a gas flow of 1 L min^{-1}, the residence time in the reactor is 0.25 s. By varying the relative composition of the nitrogen/air gas flow, the oxygen composition in the gas stream could be varied in the range 0−20%. CH_2Cl_2 was used as supplied (BDH GPR, >99% purity). No attempt was made to dry the gases. The end products of the plasma processing were monitored on-line by infrared spectroscopy using a long-path gas cell (0−10 m, Spectra-Tech) and a FTIR spectrometer (Perkin-Elmer 1710). The spectra could be transferred to a personal computer for subsequent analysis. Stainless steel, nylon, and PTFE tubing, valves, and fittings of 1/4-in. internal diameter were used to handle the gases as appropriate. The IR cell, the gas handling system, and the plasma reactor could be evacuated to remove any traces of residual gases or moisture between experiments. No attempt was made to bake or otherwise condition the surfaces of the system.

Experimental Results

A series of experiments was performed to investigate the effect of oxygen composition (0−20%) on the plasma destruction of dichloromethane and to identify the end products of the plasma processing. Figures 2 and 3 show the medium-resolution IR spectra for the end products of the plasma processing of 500 ppm of CH_2Cl_2 in pure N_2 and in 1% O_2/99% N_2, respectively.

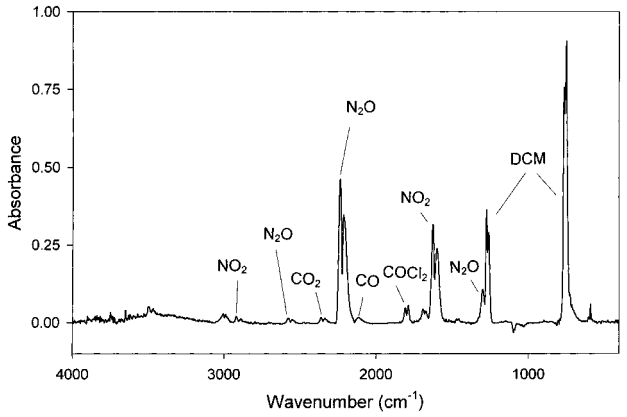

Figure 3. Medium-resolution (2 cm^{-1}) infrared spectra for an initial mixture of 500 ppm CH_2Cl_2 (DCM) in a gas stream of 1% O_2/99% N_2 at atmospheric pressure after processing in a dielectric pellet-bed reactor. The discharge conditions were $V_{pk-pk} = 15$ kV, frequency = 10.0 kHz, and flow rate = 1 L min^{-1}. The path length for the infrared gas cell was 2.12 m.

TABLE 1: Effect of the Variation of Oxygen Composition in the Gas Stream on the Plasma Decomposition of 500 ppm of Dichloromethane[a]

% O_2 in gas stream	% CH_2Cl_2 destruction	HCN	CO	CO_2	$COCl_2$	NO_2	N_2O
0	18	30	–	–	–	–	–
1	20	–	64	4	14	95	177
2	20	–	62	6	16	136	173
3	20	–	72	9	19	191	228
4	18	–	66	11	23	218	232
5	17	–	64	10	29	246	221
10	15	–	67	11	54	339	233
20	12	–	71	7	73	414	206

[a] Concentrations of end products are in parts per million.

The spectra were assigned and the measured absorbances converted into concentrations using standard compilations.[19] In the case of destruction in pure nitrogen, we see the production of only HCN, whereas CO, CO_2, NO_2, N_2O, and $COCl_2$ are detected with the presence of oxygen in the gas stream. Table 1 gives the percentage destruction of CH_2Cl_2 and the concentrations of the end products for a range of oxygen compositions of the gas stream. We did not detect any NO or HCl products, which places upper limits of ∼100 and ∼75 ppm, respectively, on the concentration of these species.

We note that, in the presence of any oxygen in the gas stream, the carbon balance is almost completely accounted for by the production of CO and $COCl_2$ and CO rather than CO_2 is formed. It should be noted that the carbon balance is overestimated in the cases of 10 and 20% O_2. In the pure nitrogen stream, the only carbon-containing end product that we can positively identify is HCN, which accounts for about one-third of the carbon balance. The only chlorine-containing end product that we detect in the oxygen-containing gas streams is phosgene, $COCl_2$, which accounts for almost all of the chlorine balance in air (20% O_2) but only ∼15% of the destroyed chlorine at a composition of 1% O_2. Given the comment above about the carbon balance, we must regard the amounts of $COCl_2$ detected in 10 and 20% O_2 as overestimates. This will be discussed below. We cannot identify any chlorine-containing end products for the destruction in pure nitrogen. The yields of $COCl_2$, NO_2, and N_2O increase with increasing oxygen content, with N_2O being the dominant oxide of nitrogen at low O_2 concentrations but NO_2 being in excess at the higher O_2 percentages.

We have recorded the current and voltage waveforms for the discharge on a fast digital storage oscilloscope (Tektronix TDS

460, 350 MHz, 100 MS/s) by using a calibrated high-voltage probe and measuring the current across a 1-kΩ resistor in the return earth path from the reactor. The current waveform shows the characteristic microdischarges composing the partial discharge. The average power is obtained by integrating the product of voltage and current as a function of time. Experience shows that this method of power determination agrees to within 5% of the results obtained using the charge−voltage Lissajous method if the sampling rate is fast enough.[20] From such measurements, we obtain an average power of 1.1 W, corresponding to an energy density of 66 J L^{-1} for a gas flow rate of 1 L min^{-1}.

Discussion

Destruction of Dichloromethane. There have been two previous studies of the destruction of dichloromethane using nonthermal atmospheric-pressure plasma methods. One by Yamamoto et al.,[9] who used a barium titanate packed-bed pellet reactor similar to that used in the present study, and a second by Penetrante et al.[14] with a pulsed corona system. Yamamoto et al. investigated the effect of voltage, initial concentration, and flow rate on the destruction of dichloromethane in dry air. Penetrante's group reports[14] the destruction of dichloromethane using a pulsed corona plasma discharge in which the carrier gas was either dry air or pure nitrogen and the gas temperature and deposited electrical energy were varied. They express the destruction in terms of a reduced parameter, β, defined by the expression

$$[X] = [X]_0 \exp(-\rho_E/\beta) \quad (1)$$

where [X] is the concentration of the volatile organic component compared with its initial concentration, $[X]_0$, for a deposited energy density of ρ_E. (ρ_E is defined as electrical power divided by gas flow.) For a gas temperature of 25 °C and an initial dichloromethane concentration of 100 ppm, they find a β value of 3170 J L^{-1} for dry air and 46 J L^{-1} for pure nitrogen. From our results in Table 1, we derive β values of 333 and 296 J L^{-1} for processing in air and nitrogen, respectively, using the dielectric pellet-bed reactor. Penetrante et al. find that the plasma processing in air becomes significantly more efficient as the gas temperature is raised (β = 1448, 545, and 46 J L^{-1} for the processing of 160 ppm of dichloromethane at 25, 120, and 300 °C, respectively). This is in contrast to their finding that, for carbon tetrachloride in air, the extent of destruction shows essentially no dependence on gas temperature. They attribute this difference to the mechanism of destruction, which involves only electron-impact processes for carbon tetrachloride, as the electron density is independent of temperature, compared with destruction by radical chemistry in the case of dichloromethane, where the increase in temperature enhances reactions with activation energy. Interestingly, the β value for the destruction of dichloromethane in nitrogen does not depend on temperature between 25 and 300 °C.

When we examine the results for the variation of oxygen content of the carrier gas, we find that there is a maximum at approximately 1−3% O_2 and that destruction is more efficient in pure nitrogen than in air. Falkenstein[6] has found similar results for the removal of trichloroethene in an O_2/N_2 mixture using a dielectric barrier discharge where the optimum destruction was obtained for an O_2 concentration of ∼2%. He attributes this behavior to a change from removal of trichloroethene by electron-impact-dominated processes, such as attachment, in pure nitrogen, through fast chlorine-induced oxidation with small amounts of oxygen, and finally to oxygen inhibition of the chlorination as the oxygen concentration of the carrier gas is further increased. Snyder and Anderson[7] reported an optimum O_2 concentration of ∼3% for the destruction of chlorobenzene with a dielectric barrier discharge in a O_2/Ar mixture. They also found that an O_2/Ar mixture was a factor of 10 times more efficient than air in the destruction of chlorobenzene, which they attribute to the "wasteful" channels forming oxides of nitrogen leaving less oxygen available for the oxidation of the chlorobenzene. They noted that, in the case of a nitrogen/oxygen mixture compared with the argon/oxygen mixture, a significant fraction of the electron energy is lost because of vibrational and dissociative excitation of the nitrogen, shifting the electron energy distribution to a lower energy region, which is less efficient for the formation of atomic oxygen by electron-impact dissociation of O_2.

Reaction Mechanism. The reaction mechanism for the high-temperature combustion of dichloromethane developed by Ho et al.[21] is initiated by unimolecular decomposition of dichloromethane to give a chlorine atom

$$CH_2Cl_2 \rightarrow CH_2Cl + Cl \quad (2)$$

followed by reaction of the chlorine with CH_2Cl_2 to give HCl.

$$Cl + CH_2Cl_2 \rightarrow CHCl_2 + HCl \quad (3)$$

The chlorinated methyl radicals produced in eqs 2 and 3 can react with O_2 to form the corresponding peroxy radicals

$$CH_2Cl, CHCl_2 + O_2 + M \rightarrow H_2ClCO_2, HCl_2CO_2 + M \quad (4)$$

which can then decompose

$$H_2ClCO_2, HCl_2CO_2 \rightarrow H_2CO, HClCO + ClO \quad (5)$$

or become stabilized and then react with themselves or other peroxy radicals.

$$H_2ClCO_2, HCl_2CO_2 + RO_2 \rightarrow H_2ClCO, HCl_2CO + RO + O_2 \quad (6)$$

These chlorinated methoxy radicals can then further react to give HCOCl and $COCl_2$.

$$H_2ClCO, HCl_2CO + O_2 \rightarrow HCOCl, COCl_2 + HO_2 \quad (7)$$

It has been suggested that reactions such as those in eqs 3−7 are also of importance for the chlorine-atom-initiated oxidation of chlorinated hydrocarbons in the troposphere.[22−24]

In the plasma, the gas is at near ambient temperature, and the electron-impact dissociation and excitation produce a range of atoms and molecules including $O(^3P$ and $^1D)$, $O_2(a^1\Delta)$, $N(^4S$, ^2D, and $^2P)$ and $N_2(A^3\Sigma_u^+)$. In the presence of atomic oxygen, dichloromethane can be removed by the relatively slow reaction

$$O + CH_2Cl_2 \rightarrow CHCl_2 + OH \quad (8)$$

The production of OH in the system allows for faster destruction of dichloromethane.

$$OH + CH_2Cl_2 \rightarrow CHCl_2 + H_2O \quad (9)$$

Further oxidation of $CHCl_2$ leads to phosgene, $COCl_2$, as discussed above.

As oxygen levels increase in the plasma, ozone formed by the recombination of oxygen atoms and molecules

$$O + O_2 + M \rightarrow O_3 + M \quad (10)$$

becomes an important reagent in the plasma processing as it has a long lifetime under the conditions of the plasma. Although we do not detect any ozone as an end product, this does not imply that it is not formed in the plasma. It may either be completely consumed between the individual discharge pulses or be decomposed during passage through the tubing and on the surface of the gas cell before detection in the FTIR spectrometer. Yamamoto et al.[9] report the detection of low levels of O_3 as an end product of the processing of dichloromethane in a pellet-bed reactor under certain conditions. This depended on the voltage applied to the reactor; the ozone concentration rose with increasing voltage to a peak and then decreased with further increase. Falkenstein[6] notes that, for low oxygen concentrations, the oxygen atoms produced in the discharge react with the volatile organic compound but, with increasing oxygen concentration, ozone will be formed and its concentration will significantly increase when all of the volatile organic compound is destroyed. We do not completely remove the dichloromethane and thus might not expect to produce ozone.

Chlorine monoxide, ClO, will be formed by the reaction of Cl atoms with ozone

$$Cl + O_3 \rightarrow ClO + O_2 \quad (11)$$

and by the reaction of excited oxygen atoms, $O(^1D)$, with dichloromethane.

$$O(^1D) + CH_2Cl_2 \rightarrow CH_2Cl + ClO \quad (12)$$

Chlorine atoms can be regenerated by the fast reaction of ClO with oxygen atoms

$$O + ClO \rightarrow O_2 + Cl \quad (13)$$

as well as with OH radicals

$$OH + ClO \rightarrow HO_2 + Cl \quad (14)$$

allowing the chlorine-atom oxidation of dichloromethane, reaction 3, to proceed in the plasma.

The reaction of oxygen and chlorine atoms with HCOCl leads to the formation of CO.

$$O, Cl + HCOCl \rightarrow CO + ClO, Cl \quad (15)$$

OH radicals will react with any HCl produced

$$OH + HCl \rightarrow H_2O + Cl \quad (16)$$

in preference to the conversion of CO to CO_2.

$$OH + CO \rightarrow CO_2 + H \quad (17)$$

Recombination of chorine atoms will produce molecular chlorine

$$Cl + Cl + M \rightarrow Cl_2 + M \quad (18)$$

suggesting that the major end products of the plasma processing in the presence of molecular oxygen will be CO, $COCl_2$, HCl, and Cl_2. We cannot confirm the production of molecular chlorine, which cannot be detected by infrared spectroscopy, and we have placed an upper limit of 75 ppm on the presence of HCl from our measurements.

In the presence of O_2 in the gas stream, we observe the formation of NO_2 and N_2O in addition to the products of the destruction of dichloromethane. NO is formed initially in the discharge by the recombination of oxygen and nitrogen atoms. NO_2 is produced from NO by several routes, including reactions with oxygen atoms, with ozone, and with the chloroperoxy radicals.

$$H_2ClCO_2, HCl_2CO_2 + NO \rightarrow H_2ClCO, HCl_2CO + NO_2 \quad (19)$$

N_2O can be produced by the reaction of N atoms with NO_2 and by the reaction of metastable N_2 with O_2.[25]

$$N_2(A^3\Sigma_u^+) + O_2 \rightarrow N_2O + O \quad (20)$$

As the concentration of O_2 in the feed gas is increased, the increase in the yield of oxygen atoms and the corresponding reduction in N atom and $N_2(A)$ concentrations will cause an increase in the production of NO_2 relative to N_2O, as we observe.

The high efficiency of destruction of chlorinated species such as CCl_4 by plasma discharges in pure nitrogen is attributed to the initial decomposition of the species by dissociative electron attachment.[1,14,6] However, electron attachment to dichloromethane is considerably less efficient than that for CCl_4 with a maximum cross section of 3.1×10^{-18} cm^2 at 300 K[26] compared with a value of 2.0×10^{-13} cm^2 for CCl_4.[27] It is known that these electron attachment cross sections increase significantly with internal excitation, and for CH_2Cl_2, the value rises to 1.7×10^{-17} cm^2 at 500 K. McCorkle et al.[28] attribute the efficient destruction of CH_2Cl_2 that they observe in low-pressure inert gas discharges to enhanced electron attachment of dichloromethane that is excited to high-lying Rydberg states by excitation transfer from the excited metastable states of the inert gases created in the discharge. However, they find lower destruction efficiencies when using nitrogen as a buffer gas and conclude that the energies of the metastable a′ and A states of N_2 are too low to be effective in the production of the high Rydberg states of CH_2Cl_2. Accordingly, we can discount dissociative electron attachment of CH_2Cl_2 as being a significant mechanism for the destruction of CH_2Cl_2 in pure nitrogen. Instead, we focus our attention on the role of electronically excited nitrogen atoms and molecules produced in the discharge. It is known[29] that $N_2(A^3\Sigma_u^+)$ will collisionally dissociate hydrocarbon molecules by excitation transfer.

$$N_2(A^3\Sigma_u^+) + CH_2Cl_2 \rightarrow N_2 + CH_2Cl + Cl \quad (21)$$

This generates chlorine atoms, allowing further decomposition of CH_2Cl_2 by reaction 3. Reaction of dichloromethane with metastable $N(^2D)$

$$N(^2D) + CH_2Cl_2 \rightarrow NCl + CH_2Cl \quad (22)$$

may contribute to the destruction of dichloromethane to a lesser extent in pure nitrogen, and the resulting CH_2Cl radicals from eqs 21 and 22 will react with nitrogen atoms to form HCN. This channel will switch off immediately in the presence of some O_2 in favor of reaction 4, and $N(^2D)$ will react with O_2 to form NO in preference to reaction 22. The NCl from reaction 22 can also react with nitrogen atoms to generate a chlorine atom.

$$N + NCl \rightarrow N_2 + Cl \quad (23)$$

TABLE 2: Mean Electron Energies and Calculated *G* Values[a] as a Function of O_2 Concentration for 500 ppm of Dichloromethane[b]

	pure N_2	1% O_2	2% O_2	3% O_2	4% O_2	5% O_2	10% O_2	20% O_2
mean electron energy/eV	3.842	3.840	3.838	3.836	3.834	3.833	3.826	3.821
process								
$e + N_2 \rightarrow N(^4S) + N(^4S, ^2D, ^2P) + e$	0.286	0.287	0.278	0.270	0.263	0.255	0.221	0.165
$e + N_2 \rightarrow N_2(A^3\Sigma_u^+) + e$	0.854	0.847	0.833	0.824	0.812	0.802	0.745	0.636
$e + O_2 \rightarrow O(^3P) + O(^3P) + e$	0	0.047	0.094	0.141	0.190	0.236	0.485	0.997
$e + O_2 \rightarrow O(^3P) + O(^1D) + e$	0	0.088	0.174	0.261	0.348	0.433	0.853	1.650
$e + O_2 \rightarrow O_2(a^1\Delta) + e$	0	0.024	0.047	0.072	0.096	0.121	0.250	0.532
$e + CH_2Cl_2 \rightarrow CH_2Cl + Cl^-$	0.00006	0.00006	0.00006	0.00006	0.00006	0.00006	0.00006	0.00006

[a] Number of reactions per 100 eV of energy deposited in the plasma. [b] Conditions: balance of N_2, temperature of 300 K, total pressure of 1 bar. The reduced electric field strength, *E*/*N*, was 150 Td. Details of the calculation and the electron-impact cross sections used are given in the text.

It is also possible that some recombination of the chloromethyl radicals occurs either with themselves or with atomic chlorine to form dichloromethane or other chloromethanes and ethanes that would be hard to detect in the infrared spectrum and these might represent the missing species in the carbon and chlorine balance (in conjunction with molecular chlorine and HCl) for the destruction in pure nitrogen. As the oxygen concentration in the feed gas is increased, the role of the nitrogen-based chemistry for the destruction of CH_2Cl_2 will be diminished, and the nitrogen species will increasingly be converted into oxides of nitrogen, thereby reducing the destruction of dichloromethane.

Determination of Active Species in the Discharge. To determine the concentrations of active species in the discharge, we have performed a solution of the Boltzmann equation to determine the electron energy distribution function from which the electron-impact rate coefficients can be generated. This was achieved using the ELENDIF computer code[30] developed to solve Boltzmann's equation for partially ionized plasmas using the appropriate electron−molecule collision cross sections for the initial gas mixture. The electron collision cross-sections for N_2 and O_2 come from the work of Phelps[31,32] and that of Pinnadawage for electron attachment to dichloromethane.[26] This gives the yields in the form of *G* values (yield per 100 eV of deposited energy) for the active species (excited- and ground-state O and N atoms and electronically excited molecular oxygen and nitrogen) produced in the discharge. The question of the yield of electronically excited nitrogen and oxygen atoms by electron impact has been discussed by Cosby[33,34] and by Zipf et al.[35] Although the production of electronically excited states by dissociation and predissociation is well established for electron energies greater than ~50 eV, there is considerable uncertainty about the yields for the lower electron energies (<10 eV) appropriate to our plasma. We have assumed that all of the states that lie above the asymptotic dissociation limits [for $N(^4S) + N(^2P, ^2D)$ and $O(^3P) + O(^1D)$] dissociate to these limits. We also assume that metastable nitrogen, $N_2(A^3\Sigma_u^+)$, is only produced directly by electron impact, although Golde[29] has pointed out that higher triplet states may contribute to the population of the A state by cascade and radiative decay. Our estimates for the yields of $N_2(A^3\Sigma_u^+)$ will then be a lower limit.

A key parameter in the solution of Boltzmann's equation is the reduced electric field strength, *E*/*N*, where *E* is the electric field and *N* is the gas density in the discharge. In a dielectric pellet-bed reactor, the concept of a uniform electric field is inappropriate, as an intense electric field is formed at the contact points of the pellets. Experimentally, dielectric plasma reactors are operated at electric fields above the minimum required for the local sustainment of the discharge and just below the point of instability giving rise to arcing. For an air plasma at atmospheric pressure, this implies a spatially and temporally averaged electric field, *E*, between 20 and 40 kV cm^{-1}, giving reduced field strengths, *E*/*N*, of approximately 75−150 Td (1 Td = 10^{-17} V cm^2). We have performed modeling of our plasma processing at the upper limit of 150 Td. The calculated *G* values are given in Table 2.

From the calculated yield values, it can be seen that dissociative electron attachment to dichloromethane is an insignificant process. There is a very small decrease in the mean electron energy of less than 1% in going from pure nitrogen to air. This is insufficient to change the nature of the electron-impact processes and the changes in the *G* values for the different processes simply reflect the changing concentrations of oxygen and nitrogen. It can be seen that the metastable $N_2(A^3\Sigma_u^+)$ is the most abundant active nitrogen species in the discharge, and we expect that the chemistry of this molecule will be significant.

Modeling of the Plasma Chemistry. The subsequent chemistry of the processing is modeled using the chemical kinetics package, CHEMKIN-II.[36] Using the method of Gentile and Kushner,[37,38] we assume that there is uniform processing of the gas as it passes through the reactor. During each half-cycle, the microdischarge current pulses create active species that then go on to initiate or continue the chemistry. In our model, a fresh supply of the active species is injected into the reaction mixture at each pulse, and the chemistry is allowed to continue until the next pulse. The concentrations of species added per pulse are determined from the *G* values calculated by the ELENDIF program and the measure of the electrical power deposited in the plasma determined above. During its passage through the reactor, the gas is subjected to 6625 such pulses at a discharge frequency of 13.25 kHz for a residence time of 0.25 s. After this time, processing ceases, and the final concentrations are output. This model is based on volume-averaged quantities. In fact, the microstreamers are filamentary in form, with diameters of approximately tens or hundreds of microns. Thus, the radicals are produced in confined regions in which there is correspondingly higher energy deposition per unit volume. Gentile and Kushner[39] have investigated the difference between a volume-averaged model and modeling more closely approximating to microstreamer dynamics for the plasma remediation of NO in air using dielectric barrier reactors. They find that, for high energy deposition, local temperature rises of several hundred Kelvin can be produced in the microdischarge and transport of reactive species in and out of the streamer can be important. Of all of the designs of dielectric barrier plasma discharge sources, the packed pellet-bed offers one in which the number of microstreamers is maximized and the volume of free gas is minimized. For this design, we feel that the volume-averaged model will provide a reasonably accurate description of the plasma processing.

A simplified reaction mechanism based on the outline given above is employed using values for the rate constants given in standard compilations[40,41] and the recent work on tropospheric

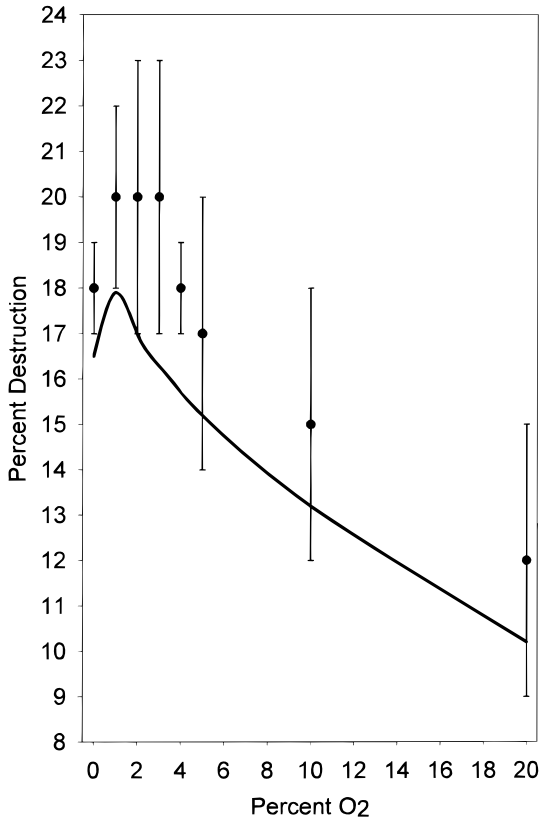

Figure 4. Comparison of the predictions (solid line) of the model for the destruction of dichloromethane as a function of the percentage of oxygen in the feed gas with the experimental results in Table 1.

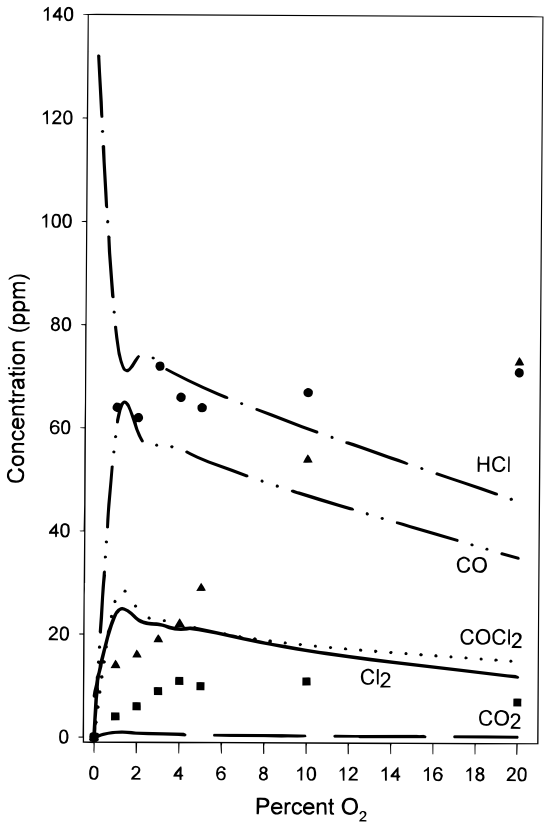

Figure 5. Comparison of the end products of the plasma processing as predicted by the model (CO_2, long dashed line; Cl_2, solid line; $COCl_2$ dotted line; CO, dashed, double-dotted line; and HCl, dashed, single-dotted line) with the experimental results for $COCl_2$ (▲), CO (●), and CO_2 (■) studied as a function of the percentage of oxygen in the feed gas. There are no experimental values for Cl_2 and HCl with which to make a comparison.

oxidation by atomic chlorine.[22,23,42] For two processes involving electronically excited atomic and molecular nitrogen, we adjusted the rate constants in order to bring the modeled levels for the overall destruction of CH_2Cl_2 into line with the experimental values. This gave $k_{21} = 2.4 \times 10^{14}$ cm^3 mol^{-1} s^{-1} and $k_{22} = 9.04 \times 10^{11}$ cm^3 mol^{-1} s^{-1}. As discussed above, reaction 22 is found to be a minor channel of importance only in the case of destruction in pure nitrogen. The value for k_{21} is at the upper end of the range of rate constants for processes involving N_2(A) but can be justified by acknowledging that a substantial proportion of the metastable nitrogen formed in the discharge will be vibrationally excited and noting that rates for collisions with N_2(A) increase rapidly with vibrational excitation of the N_2.

A comparison of the model predictions for the destruction of dichloromethane as a function of oxygen concentration with those determined experimentally is shown in Figure 4. The calculations were performed for an initial dichloromethane concentration of 500 ppm at a temperature of 300 K and a pressure of 1 atm. It can be seen that, although the calculated values lie slightly below the experimental values, the model satisfactorily predicts the initial rise in destruction efficiency observed for small amounts of added oxygen and the subsequent decrease in the destruction as the percentage of oxygen is further increased.

At a more detailed level, we can compare the model predictions for the end products with the experimental values given in Table 1. This comparison is shown in Figure 5. It can be seen that the model predicts HCl to be the major chlorine-containing end product, making up about 60% of the destroyed chlorine. The other chlorine-containing end products, Cl_2 and $COCl_2$, each account for about 20% of the destroyed chlorine. There is good agreement between the model and the experimentally determined levels of $COCl_2$ for oxygen percentages up to 5%. Beyond this level, the experimentally determined $COCl_2$ concentrations exceed the model predictions by up to a factor of 5. Given the previous comments about the carbon balances at oxygen percentages of 10 and 20%, we feel that these experimental $COCl_2$ concentrations may be in error. The model correctly reproduces the experimental observation that CO rather than CO_2 is produced, and there is reasonable agreement between model and experiment except for the concentration of CO at the highest O_2 concentrations.

The model predictions for the NO_x species are a poor representation of the experiment, with the calculated values being about an order of magnitude too low, although they correctly predict that NO_2 exceeds NO as the major NO_x species. The model suggests that the amount of N_2O produced will decrease with increasing O_2 content, in contradiction to the experimental findings. It is possible that the discrepancies have their origin in the method used to represent the plasma discharge in the model. Following Gentile and Kushner,[37] we assume a volume-averaged model in which the species are uniformly distributed throughout the volume of the reactor. In reality, the species created in the discharge are confined in space and time in the microdischarges or streamers. In this environment, the concentrations of active species are much higher, and the effective reduced electric field strengths (and possibly gas temperatures) may be much higher. Broadly speaking, the chemistry of the dichloromethane destruction is brought about by secondary radicals (which are not directly produced in the

discharge) viz. Cl, OH, HO_2, RO_2, etc. This chemistry will largely take place during the inter-pulse period when the species have diffused uniformly into the volume of the reactor. However, the NO_x-formation chemistry largely takes place because of discharge-produced radicals whose concentration falls to zero rapidly after each pulse. These processes may be poorly represented in the model. Processes that convert NO to NO_2 generally involve secondary radicals and will be well represented by the model, e.g.

$$NO + O_3, HO_2, RO_2 \rightarrow NO_2 + O_2, HO, RO \qquad (24)$$

The model also predicts the formation of ozone for the higher oxygen concentrations at the level of several hundred parts per million. We do not detect any ozone by FTIR spectroscopy. However, it should be noted that the model predicts the concentration of species as they exit the plasma reactor but detection is experimentally performed some time after the species have left the reactor and after they have been in contact with many surfaces having the potential to deactivate ozone. Thus, we cannot attach any significance to this discrepancy.

Conclusions

We have shown that dichloromethane can be efficiently destroyed in gas streams of pure nitrogen or nitrogen/oxygen mixtures by nonthermal plasma methods using a barium titanate packed-bed reactor operating at atmospheric pressure. The coproduction of NO_x species may represent a disadvantage when using oxygen-containing gas streams. The dominant mechanism for the destruction of dichloromethane is a chlorine-atom-initiated oxidation cycle in which the chlorine atoms are generated principally by collision-induced dissociation of the dichloromethane by electronically excited metastable nitrogen, $N_2(A^3\Sigma_u^+)$ and, to a lesser extent, by reaction with excited $N(^2D)$ in pure nitrogen. Because of low cross sections compared to other chlorinated species such as carbon tetrachloride, electron attachment does not play a role in the destruction of dichloromethane. The addition of small amounts of oxygen to the gas stream initially increases the destruction of dichloromethane by reactions of O atoms and OH radicals. Further increase in the O_2 concentration causes inhibition of both the chlorine-atom oxidation cycle and the formation of NO_x species and a consequent reduction in the destruction efficiency.

At high O_2 concentrations, the dominant oxide of nitrogen is NO_2 rather than NO because of the efficient conversion of NO into NO_2 by peroxyradicals. This offers the opportunity for the destruction of the NO_2 by catalytic action using, for example, a metal oxide catalyst.[43]

Acknowledgment. We acknowledge support of this work by EPSRC and AEA Technology plc under the Total Technology Scheme providing studentships for C.F. and J.J.W.

References and Notes

(1) Penetrante, B. M.; Hsiao, M. C.; Bardsley, J. N.; Merrittt, B. T.; Vogtlin, G. E.; Wallman, P. H.; Kuthi, A.; Burkhart, C. P.; Bayless, J. R. *Phys. Lett. A* **1995**, *289*, 69.

(2) Hsiao, M. C.; Merritt, B. T.; Penetrante, B. M.; Vogtlin, G. E.; Wallman, P. H. *J. Appl. Phys.* **1995**, *78*, 3451.

(3) Kohno, H.; Berezin, A. A.; Chang, J.-S.; Yamamoto, T.; Shibuya, A.; Honda, S. *IEEE Trans. Ind. Appl.* **1998**, *34*, 953.

(4) Evans, D.; Rosocha, L.; Anderson, G.; Coogan, J.; Kushner, M. *J. Appl. Phys.* **1993**, *74*, 5378.

(5) Krasnoperov, L. N.; Krishtopa, L. G.; Bozzelli, J. W. *J. Adv. Oxid. Technol.* **1997**, *2*, 248.

(6) Falkenstein, Z. *J. Appl. Phys.* **1999**, *85*, 525.

(7) Snyder, H. R.; Anderson, G. K. *IEEE Trans. Plasma Sci.* **1998**, *26*, 1695.

(8) Oda, T.; Takahashi, T.; Tada, K. *IEEE Trans. Ind. Appl.* **1999**, *35*, 373.

(9) Yamamoto, T.; Ramanathan, K.; Lawless, P. A.; Ensor, D. S.; Newsome, J. R.; Plaks, N.; Ramsey, G. H. *IEEE Trans. Ind. Appl.* **1992**, *28*, 528.

(10) Tonkyn, R. G.; Barlow, S. E.; Orlando, T. M. *J. Appl. Phys.* **1996**, *80*, 4877.

(11) Yamamoto, T.; Chang, J.-S.; Berezin, A. A.; Kohno, H.; Honda, S.; Shibuya, A. *J. Adv. Oxid. Technol.* **1996**, *1*, 67.

(12) Yamamoto, T. *J. Hazard. Mater.* **1999**, *B67*, 165.

(13) Yamamoto, T.; Mizuno, K.; Tamori, I.; Ogata, A.; Nifuku, M.; Michalska, M.; Prieto, G. *IEEE Trans. Ind. Appl.* **1996**, *32*, 100.

(14) Penetrante, B. M.; Hsiao, M. C.; Bardsley, J. N.; Merritt, B. T.; Vogtlin, G. E.; Wallman, P. H. *Pure Appl. Chem.* **1996**, *68*, 1083.

(15) Chang, J.-S. In *Non-Thermal Plasma Techniques for Pollution Control*; Penetrante, B. M., Schultheis, S. E., Eds.; Springer-Verlag: Berlin, 1993; Vol. 34, Part A, p 1.

(16) Yamamoto, T.; Lawless, P. A.; Owen, M. K.; Ensor, D. S. In *Non-Thermal Plasma Techniques for Pollution Control*; Penetrante, B. M., Schultheis, S. E., Eds.; Springer-Verlag: Berlin, 1993; Vol. 34, Part B, p 223.

(17) Mizuno, A.; Chakrabarti, A.; Okazaki, K. In *Non-Thermal Plasma Techniques for Pollution Control*; Penetrante, B. M., Schultheis, S. E., Eds.; Springer-Verlag: Berlin, 1993; Vol. 34, part B, p 165.

(18) Fitzsimmons, C.; Shawcross, J. T.; Whitehead, J. C. *J. Phys. D: Appl. Phys.* **1999**, *32*, 1136.

(19) Hanst, P. L.; Hanst, S. T. *Infrared Spectra for Quantitative Analysis of Gases*; Infrared Analysis Inc.: Anaheim, CA, 1993.

(20) Rosocha, L. A.; Anderson, G. K.; Bechtold, L. A.; Coogan, L. A.; Heck, H. G.; Kang, M.; McCulla, W. H.; Tennant, R. A.; Wantuck, P. J. In *Non-Thermal Plasma Techniques for Pollution Control*; Penetrante, B. M., Schultheis, S. E., Eds.; Springer-Verlag: Berlin, 1993; Vol. 34, Part B, p 281.

(21) Ho, W.-H.; Barat, R. B.; Bozzelli, J. W. *Combust. Flame* **1992**, *88*, 265.

(22) Hasson, A. S.; Smith, I. W. M. *J. Phys. Chem. A* **1999**, *103*, 2031.

(23) Bilde, M.; Orlando, J. J.; Tyndall, G. S.; Wallington, T. J.; Hurley, M. D.; Kaiser, E. W. *J. Phys. Chem. A* **1999**, *103*, 3963.

(24) Thüner, L. P.; Barnes, I.; Becker, K. H.; Wallington, T. J.; Christensen, L. K.; Orlando, J. J.; Ramacher, B. *J. Phys. Chem. A* **1999**, *103*, 8657.

(25) Fraser, M. E.; Piper, L. G. *J. Phys. Chem.* **1989**, *93*, 1107.

(26) Pinnaduwage, L. A.; Tav, C.; McCorkle, D. L.; Ding, W. X. *J. Chem. Phys.* **1999**, *110*, 9011.

(27) Orient, O. J.; Chutjian, A.; Crompton, R. W.; Cheung, B. *Phys. Rev. A* **1989**, *39*, 4494.

(28) McCorkle, D. L.; Ding, W.; Ma, C.-Y.; Pinnaduwage, L. A. *J. Phys. D: Appl. Phys.* **1999**, *32*, 46.

(29) Golde, M. F. *Int. J. Chem. Kinet.* **1988**, *20*, 75.

(30) Morgan, W. L.; Penetrante, B. M. *Comput. Phys. Commun.* **1990**, *58*, 127.

(31) Phelps, A. R.; Pritchard, L. C. *Phys. Rev.* **1985**, *A31*, 2932.

(32) Lawton, S. V.; Phelps, A. V. *J. Chem. Phys.* **1978**, *69*, 1055.

(33) Cosby, P. C. *J. Chem. Phys.* **1993**, *98*, 9544.

(34) Cosby, P. C. *J. Chem. Phys.* **1993**, *98*, 9560.

(35) Zipf, E. C.; Espy, P. J.; Boyle, C. F. *J. Geophys. Res.* **1980**, *85*, 687.

(36) Kee, R. J.; Rupley, F. M.; Miller, J. A. *Chemkin-II: A Fortran Chemical Kinetics Package for the Analysis of Gas-Phase Chemical Kinetics*; Sandia National Laboratory: Livermore, CA, 1991.

(37) Gentile, A. C.; Kushner, M. J. *J. Appl. Phys.* **1995**, *78*, 2074.

(38) Gentile, A. C.; Kushner, M. J. *J. Appl. Phys.* **1995**, *78*, 2977.

(39) Gentile, A. C.; Kushner, M. J. *J. Appl. Phys.* **1996**, *79*, 3877.

(40) Atkinson, R.; Baulch, D. L.; Cox, R. A.; Hampson, R. F.; Kerr, J. A.; Rossi, M. J.; Troe, J. *J. Phys. Chem. Ref. Data* **1997**, *26*, 521.

(41) Mallard, W. G.; Westley, F.; Herron, J. T.; Hampson, R. F.; Frizzell, D. H. *NIST Chemical Kinetics Database*, Windows version 2Q98; U.S. Department of Commerce, National Institute of Standards and Technology: Gaithersburg, MD, 1998.

(42) A copy of the mechanism in CHEMKIN-II format can be obtained from the authors.

(43) Hoard, J.; Wallington, T. J.; Ball, J. C.; Hurley, M. D.; Wodzisz, K. *Environ. Sci. Technol.* **1999**, *33*, 3427.